ELSEVIER

Nuclear Instruments and Methods in Physics Research A 432 (1999) 90–110

NUCLEAR INSTRUMENTS & METHODS IN PHYSICS RESEARCH Section A

www.elsevier.nl/locate/nima

The Clover: a new generation of composite Ge detectors

G. Duchêne[a,*], F.A. Beck[a], P.J. Twin[b], G. de France[a,1], D. Curien[a], L. Han[a], C.W. Beausang[b,2], M.A. Bentley[c,3], P.J. Nolan[b], J. Simpson[c]

[a]*Institut de Recherches Subatomiques, UMR 7500, CNRS-IN2P3 et Université Louis Pasteur, F-67037 Strasbourg Cedex 2, France*
[b]*Oliver Lodge Laboratory, University of Liverpool, Liverpool, L69 3BX, UK*
[c]*CLRC Daresbury Laboratory, Daresbury, Warrington, WA4 4AD, UK*

Received 2 December 1998

Abstract

This paper presents the characteristics of a new generation of composite germanium detectors: the Clover detector. Its development was based on simulation calculations performed with the code GEANT3. An extensive study of its main characteristics involving the photopeak detection efficiency, the energy resolution and the timing performed with sources and in-beam experiments have been measured. A simple Doppler broadening correction procedure is proposed to improve the in-beam energy resolution of the Clover detector. An other important property, the sensitivity to the linear polarisation of γ-rays has been measured. The performances obtained with the associated BGO suppression shield are also reported. All these results compare very well with the initial simulation calculations.

Keywords: Clover detector; Ge detectors; In-beam energy resolution; γ-rays

1. Introduction

Most of the major discoveries in the nuclear physics during the last three decades are strongly associated with detection technology innovations. In γ-ray spectroscopy the development of inorganic scintillator counters allowed the discovery in 1963 of the first excited states of a rotational band based on the ground state of ^{162}Dy [1]. A few years later, the impressive improvement in energy resolution and peak-to-background ratio obtained with semiconductor diode detectors made of germanium (Ge), lead to the first evidence of the phenomenon of backbending which is associated with a two quasi-particle excitation in ^{160}Dy [2]. Since this time, the techniques for growing Ge crystals has improved continuously and crystal sizes (diameter and length) and hence photopeak detection efficiency have increased with time. The Ge multi-detector arrays in the mid-1980s [3–5] had detection efficiency and sensitivity large enough to enable the study of nuclear structures populated by $\sim 1\%$ of the evaporation channel cross-section. An

* Corresponding author.
E-mail address: gilbert.duchene@ires.in2p3.fr (G. Duchêne)
[1] Present address: GANIL, BP 5027, F-14076 Caen Cedex 5, France.
[2] Present address: Yale University, New Haven, CT 06520, USA.
[3] Present address: Staffordshire University, Stoke-on-Trent, ST4 2DE, UK.

0168-9002/99/$ - see front matter
PII: S0168-9002(99)00277-6

example, of the power of these early arrays was the observation of the first superdeformed rotational band in 1986 in the nucleus ^{152}Dy [6] using the multidetector array TESSA 3, which is composed of 16 Compton suppressed Ge detectors [4,5]. The Ge crystals were $\sim$ 50 mm in diameter and length and the array had a total photopeak efficiency of 0.5% at 1332 keV. With the same multidetector, the existence of the intriguing phenomenon of identical superdeformed bands was observed for the first time in 1990 [7].

The next generation of arrays [8,9], e.g. GASP [10,11] and EUROGAM I [12,13] used large volume hyperpure Ge detectors (70 mm in diameter and length) and have total photopeak detection efficiencies about one order of magnitude larger than the previous spectrometers [7 and ref. therein]. This pushed the observational limit [12,14] down by about two orders of magnitude and enabled a precise and extensive study of very weak phenemona like that of identical superdeformed bands [15,16], staggering of the dynamical moment of inertia [17] and linking transitions between the super- and the normal deformed wells [18–20].

However, in 1990 when the next generation of arrays were being designed, the production of standard N-type large volume Ge crystals was somehow limited to volumes of $\sim$ 300 cm^3 and diameters of $\sim$ 70 mm. Beyond the latter value, Ge crystal production, ballistic deficit and neutron damage sensitivity problems was encountered. In addition, such large volume detectors placed around 90° to the beam direction undergo a large Doppler broadening of the γ-ray lines [8]. The realisation of new and more efficient multidetector arrays was therefore dependent on the production of new types of Ge detectors. A new concept of Ge detector was developped to overcome these difficulties: the composite Ge detector in which several crystals are assembled in a common cryostat leading to active volumes much larger than accessible with monolithic detectors. Two types of such detectors have been produced, the Clover detector [12,21–23] with four mean size crystals for EUROGAM II [9,12] and the Cluster detector [14,24] with seven encapsulated large volume crystals placed far from the target, for EUROBALL III [14]. Both have been developed in collaboration with the Company Eurisys Mesures, Strasbourg. The use of composite detectors in EUROGAM II and EUROBALL III improved substantially not only the detection efficiency but also the resolving power [14] of these arrays.

The current paper reports (i) on the detection principle of composite Ge detectors, (ii) on simulation calculations carried out with the code Geant 3 [25] to develop a new concept of composite Ge detector such as the Clover detector and (iii) on the experimental performance of the 29 Clover detectors bought for EUROGAM II.

2. The Clover detector

2.1. Ge composite detector principle

2.1.1. Main interests

The photopeak detection efficiency and the solid angle coverage that can be obtained with a composite detector is much larger than for a single-crystal detector. The granularity of a composite detector leads to interesting properties:

(i) the Doppler broadening of γ-rays emitted by recoiling nuclei can be reduced,

(ii) depending on the crystals arrangement, the composite detector can be used as a Compton polarimeter [26].

2.1.2. Detection modes

The total photopeak detection efficiency ($\varepsilon_p\omega$) of a composite detector comprising n crystals results from the sum of two complementary effects: the full γ-ray absorption in each of the individual crystals and the full γ-ray absorption in two or more crystals of the detector. The former is related to the direct detection efficiency $(\varepsilon_p\omega)_D$ and the latter to the coincidence detection efficiency $(\varepsilon_p\omega)_C$.

The direct detection efficiency $(\varepsilon_p\omega)_D$ is obtained in the direct detection mode where each crystal is used as a single detector. The composite detector is treated as n individual detectors; in this case, the linear signals of the n Ge crystals are just encoded and treated separately. Thus the detection efficiency $(\varepsilon_p\omega)_D$ corresponds to the sum of the photopeak efficiencies $(\varepsilon_p\omega)_{D,i}$ of each of the n

individual crystals:

$$(\varepsilon_p\omega)_D = \sum_{i=1}^{n} (\varepsilon_p\omega)_{D,i}. \quad (1)$$

The second component $(\varepsilon_p\omega)_C$ is measured in the coincidence detection mode which is triggered only when two or more crystals are in temporal coincidences. Beside eventual multiple hits, the coincidence events are mainly related to Compton scatterings from one crystal to its neighbours. The initial energy E_γ of the γ-ray detected is partially deposited in the j individual crystals firing: E_γ is recovered by summing the $E_{\gamma,j}$ partial energies when a full absorption event occured in the composite detector. In practice, the energy signals of the crystals that are hit simultaneously are recorded in an event-by-event mode and treated off-line.

As the coincidence photopeak detection efficiency $(\varepsilon_p\omega)_C$ has to be added to the direct photopeak efficiency $(\varepsilon_p\omega)_D$ to obtain the total photopeak efficiency $(\varepsilon_p\omega)$, it is also called add-back photopeak efficiency $(\varepsilon_p\omega)_{AB}$. We will keep the latter labelling for the following discussions.

The total detection efficiency can be written as

$$(\varepsilon_p\omega) = (\varepsilon_p\omega)_D + (\varepsilon_p\omega)_{AB} \sim n(\varepsilon_p\omega)_{D,1} + (\varepsilon_p\omega)_{AB}. \quad (2)$$

The approximation in Eq. (2) applies when the different crystals of the composite detector have about the same efficiency, e.g. the same sizes and shaping.

During the off-line analysis, the direct and the add-back modes are analysed simultaneously to get the best performance of the composite detector. This simultaneous treatment (direct + add-back) is called the total detection mode.

2.2. Clover Ge detector geometry

The Clover detector consists of four coaxial n-type Ge diodes of 50 mm diameter and 70 mm length mounted in a common cryostat. Each crystal is shaped as shown in the upper left panel of Fig. 1. The front face has a quasi-squared section obtained by bevelling two adjacent faces with an angle of 7.1° starting at around the half of the crystal length and by cutting the two remaining faces parallel to the crystal axis along its whole length. This enables a close packing of the diodes with a Ge–Ge distance of only 0.2 mm (upper right panel of Fig. 1). The total active Ge volume is ~ 470 cm^3 and corresponds to 89% of the original Ge volume. In order to optimise the signal-to-noise ratio of the composite detector, the aluminium housing generally used to hold the crystals is replaced by a grip that holds the diodes by their rear side. The distance between the beveled edges of the crystals and the internal surface of the end-cap is only 3.5 mm. The thickness of the aluminium end-cap is 1.5 mm. A common ground (high voltage) is applied on the outer (inner) contacts of the diodes. The energy signal is collected for each crystal from the inner contact via AC-coupling.

3. Monte-Carlo simulation calculations

The ability of the GEANT code [25] which uses the Monte-Carlo technique to predict Ge detector performance, has been demonstrated by the calculation of the photopeak detection efficiency at 1332 keV for several Ge detectors of different types and volumes [27]. The results of the calculations were compared with the corresponding measured values. The differences between simulation calculations and measurements were reduced to less than 2% over a large set of Ge detectors allowing us to be very confident in our future predictive simulation calculations [27].

Such simulation calculations have been consequently performed to determine the performance of a composite detector like the Clover detector. They allowed us to define its final geometry by optimising its response function. Beside the principal characteristic, the photopeak detection efficiency, we have also calculated the peak-to-total ratio with and without Compton suppression and studied the multiple Compton scattering in the composite detector. We have also simulated the in-beam deterioration of the energy resolution due to Doppler broadening and determined a simple correction method based on the granularity of the Clover detector and the multiple Compton scattering probabilities.

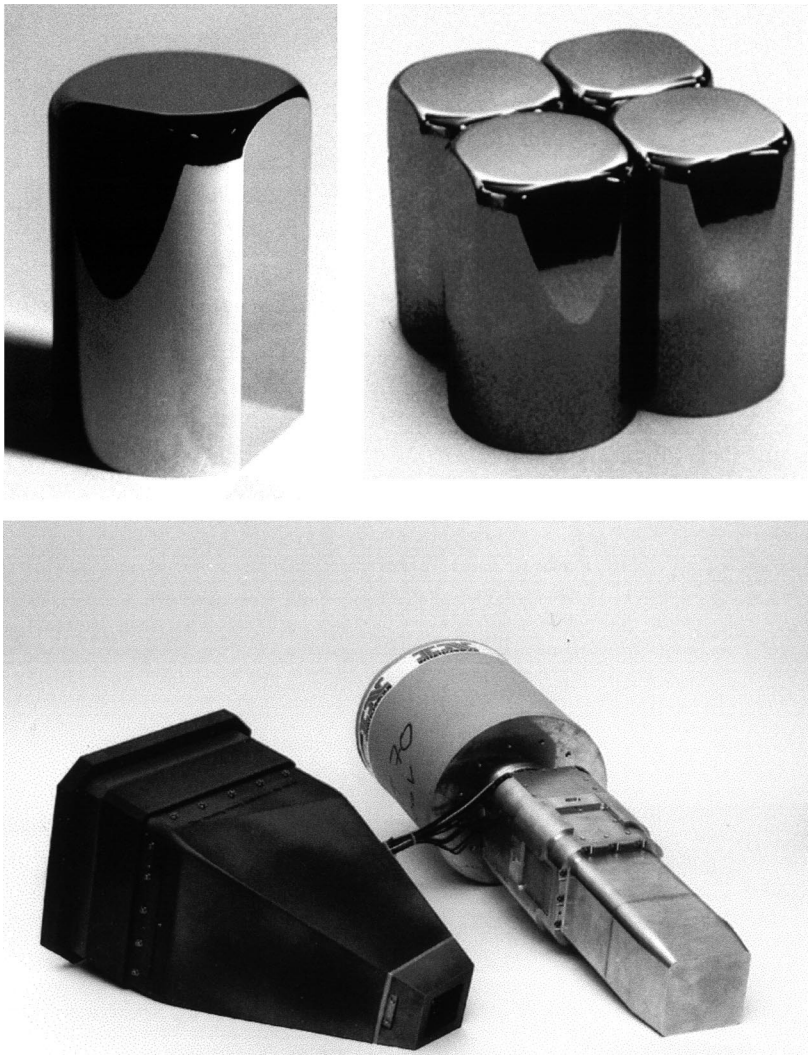

Fig. 1. Upper left panel: individual Clover crystal. Upper right panel: close packing of the four shaped Ge crystals of a Clover detector. Bottom panel: the Clover detector (right hand side) and its escape suppression shield (left hand side)

3.1. Design

Because the geometry of the Clover detector is rather complex, it was not possible to reproduce it exactly using the elementary volumes defined in the GEANT's catalogue. For example, the bevels at the front face of each diode generate, on the side, a semi-elliptic surface which was not reproducible in the calculations. Therefore, some geometrical approximations were needed. To stick as close as possible to the real situation, we decided to conserve the most important parameters and to alter some others. The conserved quantities are the total volume of Ge, the full length of the crystals, the tapered angle and the surface of the Ge front face, i.e. the solid angle. As a consequence, the dimensions of the rear section of the Clover detector were modified. The simulated shape consists in

a squared-based pyramid truncated at the front (which corresponds to the beveled length) and in a parallelepipedic box at the rear. In this simulated volume, the coaxial hole of each diode and the dead materials such as the implanted lithium contact, the holding structure in aluminium and an additional aluminium block corresponding to the cold electronics at the rear of the crystals were included. This detector is then mounted in a 1.5 mm thick aluminium can.

The BGO escape suppression shield is more straightforward to reproduce as it can be modeled with tapered trapezoids. The calculations for the BGO scintillator did not include the light collection process.

3.2. Calculated performances

To enable a realistic comparison of calculated and experimental Ge performances, the detector was simulated at the same source or target to Ge front face distance, angle to the beam axis, positionning in the suppression shield, etc. Both the experimental and simulated performances are reported in Sections 4 and 5.

The experimental values of the photopeak detection efficiency and the peak-to-total ratio, as well as the results of the simulation calculations performed at 1332 keV for the Clover geometry defined in Section 2.3, are reported in Table 1. A remarkable agreement between the two sets of values is found with differences less than 3%.

We have calculated the distribution of the number of individual crystals which have fired when a single 1332 keV γ-ray is fully detected in the Clover detector. The distribution shows that $\sim 1/3$ of the full absorption events have triggered more than one diode. This indicates that a large proportion of photopeak events consists of scattered events involving several Ge crystals (see Table 1).

The in-beam Doppler broadening of the γ lines has also been calculated. In the next sub-section, we define a simple Doppler shift correction method which uses the subdivided structure of the Clover detector to strongly improve the in-beam energy resolution.

Table 1
Calculated and measured characteristics of Clover detectors obtained at 1332 keV: absolute photopeak efficiency and peak-to-total ratio in total detection mode, add-back factor F and distribution of the number of firing crystals for full absorption events

Characteristics	Calculated	Measured
$\varepsilon_p\omega$	16.3×10^{-4}	$16.1(5)\times10^{-4}$
P/T	0.29	0.30 (1)
F	1.52	1.53 (1)
Single	65.9 %	65.3 (2) %
Double coinc.	30.8 %	30.8 (1) %
Triple coinc.	3.3 %	3.7 (1) %
Quadr. coinc.	—	0.2 (1) %

3.3. Doppler broadening correction principle

The Clover detector used in a multidetector array with a distance Ge-to-target of approximately 20 cm, subtends a large solid angle Ω ($\omega = \Omega/4\pi \sim 10^{-2}$). A large Doppler broadening effect is therefore expected which strongly reduces the resolving power of the array. The latter quantity is proportional to the average in-beam peak-to-total ratio and inversially proportional to the average in-beam energy resolution of its detection units [8,14]. Such a unit corresponds to the Ge detector and its Compton suppression shield. The energy resolution results from the quadratic summation of four components [28]:

- the intrinsic energy resolution of the Ge detector,
- the broadening related to the slowing down in the target of the γ emitters,
- the broadening due to the angular spread of the recoils,
- the Doppler broadening due to the opening angle of the Ge detector.

Numerical examples of the relative weight of the different in-beam FWHM components are given in Ref. [28] versus the detector angular position to the beam axis.

The intrinsic FWHM of the large volume Ge counters is very good typically below 2.1 keV (2.4 keV) for a shaping time constant of 6 μs (3 μs) at 1332 keV.

The recoils slowing down can be reduced by use of a stack of thin targets.

The influence on the FWHM of the angular spread of the recoils is large at angular positions θ close to the beam axis ($\theta \sim 0^\circ$ and 180°). This effect is only partially corrected by the direct detection of the recoils in a detector located at forward angles which determines the recoil direction [29] or, when the evaporation channel involves at least one p or α particle, by a kinematical reconstruction based on the detection of the evaporated charged particles [30].

The opening angle of the detector produces the largest FWHM alteration at angles around 90° to the beam axis.

Therefore the detector opening angle is the main concern in the design of a γ multidetector. This explains our choice, to build the Clover detector, to use a relatively small diameter for the individual diodes.

This was also one of the main reasons why the Clover detectors were developped for the EUROGAM II spectrometer. In this array there are 24 Clover detectors in two rings of 12 counters at 75.5° and 104.5° to the beam direction. The front face of the Ge crystals is 23 cm from the target in this geometry.

To calculate the Doppler broadening of the γ-ray line shapes for γ transitions emitted from a moving source, we have taken into account the four FWHM components listed above. The nuclear reaction conditions were those of a typical experiment for the study of superdeformed bands in the mass region $A \simeq 150$. The intrinsic energy resolution of the Ge detector is defined as a linear function of the γ-ray energy (1.3 at 122 and 2.3 keV at 1.33 MeV). The opening angle reduced by the heavy metal collimator was used for each individual Ge diode of the Clover detector. The half recoil angle was calculated to be $\sim 6.5^\circ$.

The simulated events were generated using this set of parameters. At the end of the process of each event, the detected γ-ray energies were corrected according to the Doppler shift calculated from the experimental conditions.

From the simulation calculations [21] we have deduced that, for photopeak events resulting from the coincidence between two Clover crystals, more than 75% of the events corresponds to Compton scatterings with a first interaction point located within ± 20 mm around the surface separating the firing diodes. This effect is almost γ-ray energy independent. The calculated distributions of the first interaction point of such events are presented in Fig. 2 for incident γ-ray energies $E_\gamma = 200,1332,$ and 5000 keV. The ± 20 mm region is shown by the vertical dashed lines. All three distributions look very similar and are centred on the separation surface between the firing diodes. Consequently we

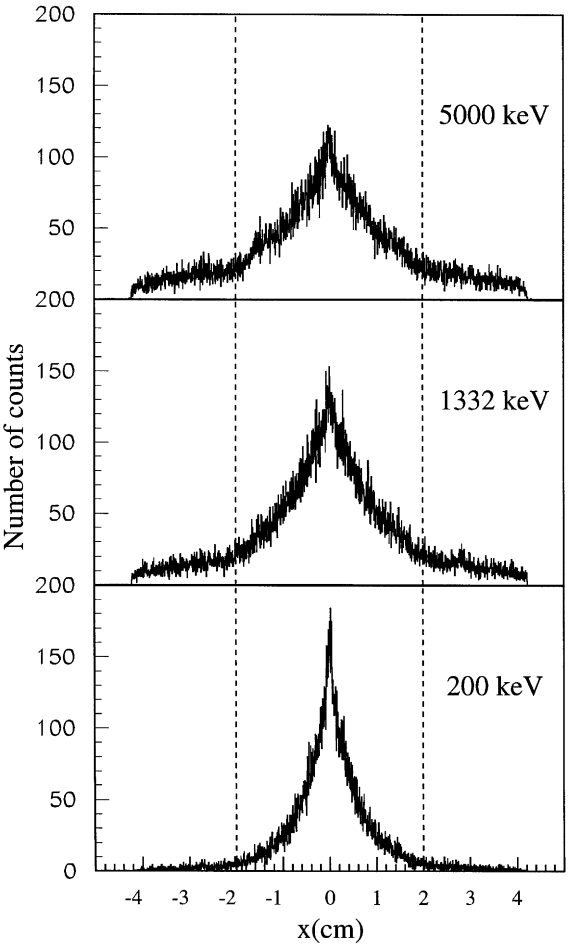

Fig. 2. Compton scattering events between two adjacent Clover crystals. Spacial distributions of the first interaction point around the surface separating the firing crystals calculated for γ-ray energies of 200, 1332 and 5000 keV. The dashed lines defines the ± 20 mm interaction region.

have developped and tested a new Doppler shift correction procedure adapted to the Clover detector:

- the composite detector is divided perpendicular to the beam axis in two halfs of two crystals,
- whenever a γ-ray fires one of the diodes of a Clover half or scatters between the two crystals of a half, the angular position used for the Doppler shift correction is the angle θ of the Clover half hitted which is called the "half angle",
- when a γ-ray scatters between the two Clover halfs, the angle used is the central angle of the Clover detector called the "Clover angle".

This new Doppler shift correction procedure uses three angles, the two half angles and the Clover angle. The experimental results reported in Section 5.3 will show the efficiency of this simple method.

4. Source measurements

The present section reports on the measurements of the intrinsic characteristics of the Clover detector performed for different γ-ray energies. The peak-to-background improvement obtained with a BGO Compton suppression shield is also discussed.

4.1. Experimental conditions

The measurements of photopeak detection efficiencies, add-back factor and energy resolution have been performed, using several γ-ray sources ^{60}Co, ^{152}Eu, ^{133}Ba and ^{56}Co. The Clover performances in the direct and the total detection modes (direct + add-back modes) was deduced in an off-line analysis versus γ-ray energy. The detector was placed vertically with the crystals at a distance larger than 1.5 m from floor and walls to reduce the contribution of back-scattered γ-rays from the environment. A very thin plexiglas source holder, centred along the Clover detector axis, was placed at a distance of 25 cm from the Ge crystal front face. The sources used had activities of about 10 μCi leading to a counting rate of a few kHz in the total detection mode. Energy and timing signals were taken from each crystal. Spectroscopy amplifiers with Gaussian shaping and a shaping time constant of 4 μs were used. The 8 K ADCs were triggered by an OR of the CFD's outputs of the four crystals. The data were recorded on tape in an event-by-event mode.

4.2. Add-back factor and detection efficiency

4.2.1. Definitions

The normalised solid angle ω of a detector corresponds to the solid angle Ω sustained by the counter normalised to 4π str ($\omega = \Omega/4\pi$).

The photopeak efficiency $\varepsilon_p\omega$ (E_γ) of a detector is the product of the intrinsic photopic efficiency $\varepsilon_p(E_\gamma)$ by the normalised solid angle ω. The parameter ε_p, generally given at 1332 keV, cannot be measured directly; it is deduced from the measured quantity $\varepsilon_p\omega$, the normalised solid angle ω being calculated. The latter quantity depends on the measurement geometry, distance D between the Ge front face and the source, sizes and shape of the Ge crystal. A precise calculation of ω is essential to extract the proper ε_p value.

The EUROGAM I multidetector was composed of 45 tapered Ge detectors surrounded each by a BGO suppression shield [12,13]. The tapered detector consists of a cylindrical crystal of 70 mm in diameter and length and presents a conical bevel ($\theta = 5.9^\circ$) along 3 cm from the front face.

For the tapered detectors, ω can be calculated with the following expression:

$$\omega = \frac{1}{2}\left(1 - \sqrt{\frac{D^2}{D^2 + r^2}}\right) \tag{3}$$

where r is the radius of the Ge front face. In the case of the Clover detector, its complex geometry leads to an integral equation of the solid angle which has been calculated numerically.

For a composite detector, the total photopeak efficiency $\varepsilon_p\omega$ is enhanced as compared with the photopeak efficiency in the direct detection mode $(\varepsilon_p\omega)_D$ by the add-back contribution $(\varepsilon_p\omega)_{AB}$ (see Eq. (2)). The total photopeak efficiency $\varepsilon_p\omega$ can be written as the product of $(\varepsilon_p\omega)_D$ by the add-back factor F:

$$\begin{aligned}\varepsilon_p\omega &= (\varepsilon_p\omega)_D + (\varepsilon_p\omega)_{AB} = (\varepsilon_p\omega)_D \times [1 + f] \\ &= (\varepsilon_p\omega)_D \times F\end{aligned} \tag{4}$$

where the addition factor f is given by

$$f = \frac{(\varepsilon_p \omega)_{AB}}{(\varepsilon_p \omega)_D} \quad (5)$$

and the add-back factor $F = 1 + f$ is larger or equal to one.

The peak-to-total ratio P/T corresponds to the sum of the ^{60}Co net peak areas divided by the total number of counts in the spectrum for energies from 100 to 1350 keV.

4.2.2. Standard measurements at 1332 keV

Table 1 compares various calculated and measured characteristics of the Clover detector obtained with a ^{60}Co source at 1332 keV. There is an excellent agreement between the calculated and the measured data. This table shows that at 1332 keV:

(i) the total detection efficiency is increased by 50% relative to the direct detection efficiency due to the contribution of the Compton scattered coincidences, the γ-rays being fully absorbed in the total Ge volume,

(ii) most of the coincidences correspond to Compton scattering between two crystals.

Note that the diagonal double coincidences and the triple coincidences amount to about the 11th and the 10th of the double coincidences events, respectively.

Table 2 reports the mean values of several characteristics obtained in direct and total detection mode with the 29 Clover detectors delivered by Eurisys Mesures Company to the EUROGAM collaboration. The Ge photopeak efficiencies given in percent are normalised to the photopeak efficiency of a 7.6 cm × 7.6 cm NaI(Tℓ) scintillator at 1332 keV (12.44×10^{-4} absolute efficiency at 25 cm) measured in the same experimental conditions.

The uncertainties on the relative efficiencies reported in Tables 1 and 2 (∼ 3%) are mainly due to the contribution of the relative uncertainty of the initial ^{60}Co source activity (2.5%). The accuracies of the add-back factor, the peak-to-total and the coincidences distribution include only statistical errors as all these quantities are ratios or percentages.

The average relative efficiency of a single Clover diode (21.3 (6)%) compares fairly well with the calculated efficiency: 21.6%. In the total detection mode the measured relative efficiency for the Clover detector is, on average, 130 (4)% at 1332 keV. The experimental add-back factor is 1.53 (2). The distribution around the mean value of the relative photopeak efficiency for the 29 Clover detectors is quite narrow (123–139%).

The comparison between the average relative photopeak efficiencies of the Clover detector (130%) and the monolithic tapered detector of EUROGAM I (73%) shows a gain in detection efficiency by a factor 1.8 [21–23]. As this impressive result refers to the photopeak efficiency $\varepsilon_p\omega$, it is also interesting to compare the intrinsic photopeak efficiencies ε_p of both types of detectors.

From the experimental absolute photopeak efficiency values, measured at $D = 25$ cm, we have extracted the intrinsic photopeak efficiencies for both the tapered ($\varepsilon_{p,tap}$) and the Clover ($\varepsilon_{p,clo}$) detectors.

Table 2
Relative photopeak efficiency at 1332 keV, peak-to-total ratio P/T (see Section 4.2.1) energy resolution at low (122 keV) and high (1332 keV) energies and timing response of the individual Clover crystals and of the Clover detectors in the total detection mode averaged over the 29 Clover units produced for EUROGAM II. The timing is measured versus a BaF_2 scintillator for the individual crystals and between two Ge crystals for the Clover detectors. The conditions for the timing measurements are given in the text, Section 4.4

Average response	$\varepsilon_p\omega$ (1332 keV) (%)	P/T	FWHM (122 keV)	FWHM (1332 keV)	Timing resolutions (ns)
Individual crystals	21.3 (6)	0.16 (1)	1.03 (2)	1.95 (5)	5.5 (5)
Clover detectors	130 (4)	0.30 (1)	1.03 (2)	2.11 (5)	8.0 (5)

We have determined from the relative photopeak detection efficiencies of 50 tapered detectors a mean value of $\varepsilon_p\omega = 73.0\,(2)\%$. As the front face radius is $r = 3.25(6)$ cm, we get the following values by use of Eq. (3):

$$\omega_{tap} = 4.20(15)\times 10^{-3} \quad \text{and} \quad \varepsilon_{p,tap} = 0.216(8).$$

The calculated normalised solid angle and intrinsic efficiency of a bare Clover detector in the total detection mode are:

$$\omega_{clo} = 8.01(12)\times 10^{-3} \quad \text{and} \quad \varepsilon_{p,clo} = 0.202(7).$$

We observe that the intrinsic photopeak efficiency for the Clover detector is slightly smaller than that of the tapered counter. Therefore, the fact that the photopeak detection efficiency of the composite detector is larger by a factor ~ 1.8 over the tapered one is only due to the difference in solid angle ($\omega_{clo} \sim 1.9\omega_{tap}$). The increase of the intrinsic photopeak efficiency from 0.132(4), the value for the individual Clover diodes, to $\varepsilon_{p,clo}$ corresponds in fact to the add-back factor value, 1.53. This underlines that the largest intrinsic photopeak efficiency of a composite detector will be reached when using large ε_p individual diodes. However due to its large solid angle, the use of the Clover detector in a 4π array increases the Ge versus BGO solid angle coverage which finally leads to a gain in the photopeak detection efficiency of the multidetector with several advantages related to the Clover granularity.

4.2.3. Variations versus γ-ray energy

Fig. 3 shows the measured absolute photopeak efficiencies for the direct detection mode (open squares), the double coincidences (full stars) and the total detection mode (full circles) of a Clover detector. Is also presented the photopeak detection efficiency of a tapered detector (full line).

The slope of the efficiency curves versus the γ-ray energy is to be related to the intrinsic photopeak efficiency of the detector. Therefore the quite downsloping curve in the direct detection mode (open squares) corresponds to $\varepsilon_p \sim 0.13$. The quite parallel slopes for the tapered (full line) and the Clover detector in the total detection mode (full circles) reflects similar $\varepsilon_{p,tap}$ and $\varepsilon_{p,clo}$ values.

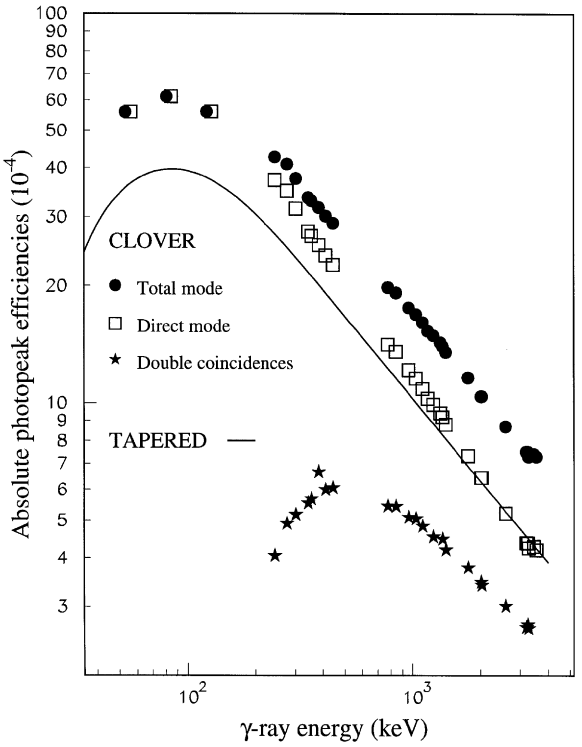

Fig. 3. Absolute photopeak efficiencies for the direct detection mode (open squares), the double coincidences (full stars) and the total detection mode (full circles) of a Clover detector versus γ-ray energy. The photopeak efficiency of the EUROGAM I tapered detector (full line) is also shown

At γ-ray energies lower than 130 keV, the photopeak efficiencies in direct and total detection modes are identical. This means that the add-back factor F is constant and equals 1 ($f = 0$) over the 0–130 keV range. At so low energy the Compton scattering cross-section is very small and the γ-ray absorption is dominated by the photoelectric effect.

At higher energies, the addition factor f varies linearly versus the logarithm of the γ-ray energy as shown in Fig. 4. The fit of the experimental data leads to the following expression with E_γ in keV:

$$F(E_\gamma) = 1 + f(E_\gamma) \quad \text{where } f(E_\gamma)$$

$$= \begin{cases} 0.221(3).\ell n(E_\gamma) - 1.07(2), & E_\gamma \geq 130\,\text{keV} \\ 0, & E_\gamma < 130\,\text{keV}. \end{cases} \quad (6)$$

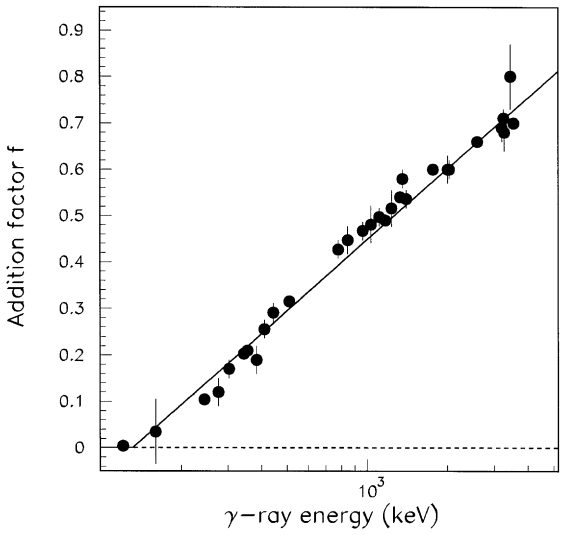

Fig. 4. Addition factor f for the Clover detector versus γ-ray energy.

4.3. Energy resolution

The energy resolution of a detector corresponds to the full-width half-maximum (FWHM) of the lines in a γ spectrum obtained with this counter. The average FWHM at 122 and 1332 keV of individual crystals, measured with a Gaussian shaping time constant of 4 μs are reported in Table 2 as well as the mean values obtained for the Clover detector in the total detection mode.

The 1.03 keV FWHM measured at 122 keV is related to the large capacitance of the individual crystals due to their length and shaping ($\sim$ 42 pF as compared with $\sim$ 25 pF for cylindrical crystals of 50 mm diameter and 50 mm length). Due to the relatively small diameter of the individual Clover crystals, no ballistic deficit [31] is observed at 1332 keV so that even with a shorter shaping time constant of 2 μs, usually used in in-beam experiments, the FWHM remains good ($\sim$ 2.2 keV).

The energy resolution of the Clover detector in the total detection mode is only weakly deteriorated relative to the direct detection mode (see Table 2). The FWHM of the Clover detector at 122 keV is of course not modified ($f = 0$) and only a small increase of $\sim$ 8% at 1332 keV is observed. To better explain this remarkable property, we performed a FWHM measurement versus γ-ray energy with a ^{152}Eu source. The data are presented in Fig. 5 where the squared measured energy resolutions in direct mode (open circles), in add-back mode (sum of all coincidence events; crosses) and in total detection mode (full circles) are shown versus the γ-ray energy. The energy resolutions have been fitted for the direct and the add-back modes and calculated for the total detection mode. The results of the fits and calculations are also shown in Fig. 5. The theoretical expressions are derivated below.

The energy resolution of a composite detector in the direct detection mode is identical to the one of a classical semiconductor detector as a function of the γ-ray energy. When the charge collection process is not affected by carrier trapping or ballistic deficit, the FWHM of a peak can be written as:

$$\mathrm{FWHM}^2 = N^2 + \alpha E_\gamma \tag{7}$$

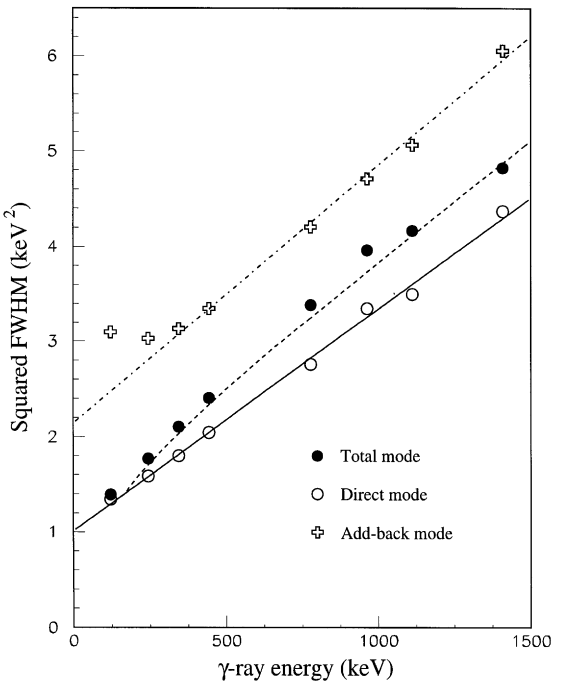

Fig. 5. Squared energy resolution versus γ-ray energy. The experimental (calculated) FWHMs in direct, add-back and total detection modes (respectively open circles (full line), crosses (dashed-dotted line) and full circles (dashed line)) are shown for the Clover detector.

where in the first term N is the crystal and preamplifier noise contribution and the second term is the charge collection term in which α is a scaling coefficient.

The detection of a γ-ray in the add-back mode implies the simultaneous triggering of m crystals (for a Clover detector $2 \leq m \leq 4$). The summation of the partial γ-ray energies deposited in the m segments leads to the summation of the noise of each of the m linear channels. Assuming that the four crystals are identical, the noise N^2 in Eq. (7) has to be replaced by mN^2 for an m-fold event.

The energy resolution in the total detection mode, $\mathrm{FWHM}_{\mathrm{total}}$, for a given γ-ray energy E_γ involves the contribution of single events and double, triple and quadruple coincidences. Thus the m-fold FWHM expressions are to be summed, weighted by their probability of occurence P_m. We find

$$\mathrm{FWHM}^2_{\mathrm{total}} = \sum_{m=1}^{4} P_m(mN^2 + \alpha_m E_\gamma). \tag{8}$$

As in a wide γ-energy range most of the coincidences are doubles, expression (8) simplifies to

$$\mathrm{FWHM}^2_{\mathrm{total}} = \frac{1}{F}(N^2 + \alpha_1 E_\gamma) + \left(\frac{F-1}{F}\right)(2N^2 + \alpha_2 E_\gamma). \tag{9}$$

The coefficients $1/F$ and $(F-1)/F$ are the P_m probabilities for $m = 1$ and $= 2$, respectively.

The experimental data fitted using Eq. (8) to extract the values of the mN^2 and α_m parameters for single events and multiple coincidences are given in Table 3. The corresponding curves are shown in Fig. 5 (full and dashed-dotted curves for, respectively, single and coincidence events). Using data in Table 3 and Eq. (6) for the add-back factor, the energy resolution in the total detection mode is calculated with Eq. (9) and shown by the dashed line in Fig. 5. Good agreements between the experimental and calculated values are obtained.

When comparing the averaged performances of the Clover detectors in the total detection mode with the large monolithic tapered detectors mounted in EUROGAM I, the energy resolutions are similar at 1332 keV (2.11 and 2.10 keV, respectively). The FWHM of the composite detector is even slightly better than for tapered detectors for higher γ-ray energies. Therefore the Clover detector is an excellent tool for the spectroscopy of nuclear structures deexciting via high γ-ray energy transitions.

Table 3
Experimental values of mN^2 and α_m fitted on the data shown in Fig. 5 for one of the Clover detectors in direct and in add-back modes. The values for the tapered detector are extracted from mean FWHM values measured at 122 keV (935 eV) and 1332 keV (2.10 keV)

	Clover		Phase 1
	$m = 1$	$m > 1$	
mN^2 (keV^2)	1.01 (3)	2.13 (5)	0.517 (5)
α_m (keV)	2.33 (4) $\times 10^{-3}$	2.7 (1) $\times 10^{-3}$	2.9 (4) $\times 10^{-3}$

4.4. Timing characteristics

Using a ^{60}Co source the timing performance of each Clover crystal (Table 2) has been measured in coincidence with a small BaF_2 scintillator whose timing resolution is ~ 500 ps. Pulses from both counters were processed using standard NIM timing filter amplifiers (TFA) and, for the Ge detector, a CFD. An external delay of 35 ns and a threshold of 50 keV was used for the Ge CFD and integration and differentiation constants of 0 and 200 ns, respectively, were applied in the TFA. The coincidence time spectrum, generated by a time to amplitude converter (TAC) was recorded with a multichannel analyser. The start and stop signals were derived from the scintillator and the Clover crystal, respectively. In these measurements the source was placed at a distance of approximately 5 cm from the Ge crystals along the composite detector axis which gave a rate of about 2 kHz in each diode. For the BaF_2–Ge coincidences, we obtained a timing peak FWHM of 5.5 ns with a classical Lorentzian shape (FWTM/FWHM $\sim$ 3 for γ-ray energies larger than 50 keV). When a coincidence between two Ge crystals was required, the timing FWHM was 8.0 ns.

4.5. Peak-to-total ratio

Peak-to-total values P/T obtained with unsuppressed data are given in Table 2. A substantial improvement of P/T is observed between the direct and the total detection modes (0.16 and 0.30, respectively). The latter result is in good agreement with the simulation calculations (see Table 1). The value in the total detection mode ($P/T = 0.30$) is larger than that obtained with the tapered detector, which is typically of about 0.25 [13].

4.5.1. The Compton suppression shield

In EUROGAM II the composite detector is surrounded by a symmetric Compton suppression shield (see Fig. 5 of Ref. [32]) which consists of 16 optically isolated trapezoidal BGO crystals, each fitted with a photomultiplier tube (see bottom panel in Fig. 1). The length of each crystal is 242 mm while its thickness varies from 19.5 mm at the back to about 3 mm at the front of the shield. High voltage is applied separately to each phototube. The PMT output signals are coupled in pairs. A 35 mm thick heavy-metal collimator is used to prevent the firing of the BGO crystals by direct radiations from the target.

Typically, for each BGO crystal the energy resolution obtained at 662 keV is $\sim 19\%$ and the peak-to-valley ratio at 60 keV (^{241}Am) is about 6 for a source centered inside the shield. The timing characteristics of the BGO crystals has been measured with a ^{60}Co source in coincidence with a small BaF_2 scintillator. The FWHM and the FWTM are respectively 3.7 and 9.3 ns. The BGO-BGO timing response is of about 7 ns FWHM.

The front face of the Ge crystals is positioned 6 cm behind the front of the shield crystals to allow a good suppression of backscattered events from the Ge.

4.5.2. Compton suppression performance

The data presented in this section were obtained with a ^{60}Co source placed far from any material at 230 mm from the front face of the Ge crystals (EUROGAM II geometry, see Section 5). The BGO CFD thresholds were set just above the noise at about 15 keV. All spectra from which results were obtained, were background subtracted.

The unsuppressed and suppressed spectra for ^{60}Co, shown in Fig. 6, were obtained with the Clover detector operating in the total detection mode. The suppressed P/T ratio (see Section 4.2.1) is measured to be 0.55, a value comparable with the one obtained for the tapered counter in its suppression shield ($P/T = 0.57$ see Ref. [13]). The suppressed spectrum is quite flat between 400 and 900 keV. However, it shows structures typical of the suppression of symmetric anti-Compton shields: the sharp Compton edges due to missed backscattering from the Ge crystal and a low-energy bump generated by backscattering from the copper cold finger of the cryostat placed behind the Ge crystal. By comparing channel by channel the Compton background of the suppressed and unsuppressed spectra, a background reduction by a factor 2 to 5 versus γ-ray energy is observed. An indication of the quality of the suppressed spectrum is given in the insert of Fig. 6.

5. In-beam tests with EUROGAM II

5.1. EUROGAM II and experimental conditions

The multidetector array EUROGAM II consists of three sections, two end caps for the tapered large volume Ge detectors placed at a distance D of 20.5 cm from the target and a central section for the Clover detectors ($D = 23$ cm) [12]. The tapered Ge counters are located in four rings, 5 at 22.4° (157.6°) and 10 at 46.4° (133.6°) to the beam direction for the forward (backward) end caps. The Clover detectors are mounted in two rings of 12 counters at 75.5° and 104.5°.

In EUROGAM II the collimation reduces the edges of the Clover squared front face by 6 mm. The Clover normalised solid angle in the array is therefore $\omega_{clo} = 8.38 \times 10^{-3}$. Using the intrinsic photopeak efficiency $\varepsilon_{p,clo}$ determined in Section 4.2.2 at 1332 keV, we get for the Clover section a photopeak efficiency of 4.1%. This result is in fair agreement with the photopeak efficiency of 4.0 (2)% measured for the Clover section and the value for the whole array of 7.35 (4)% [23].

All data presented in this section refer to mean values obtained with the composite counters from

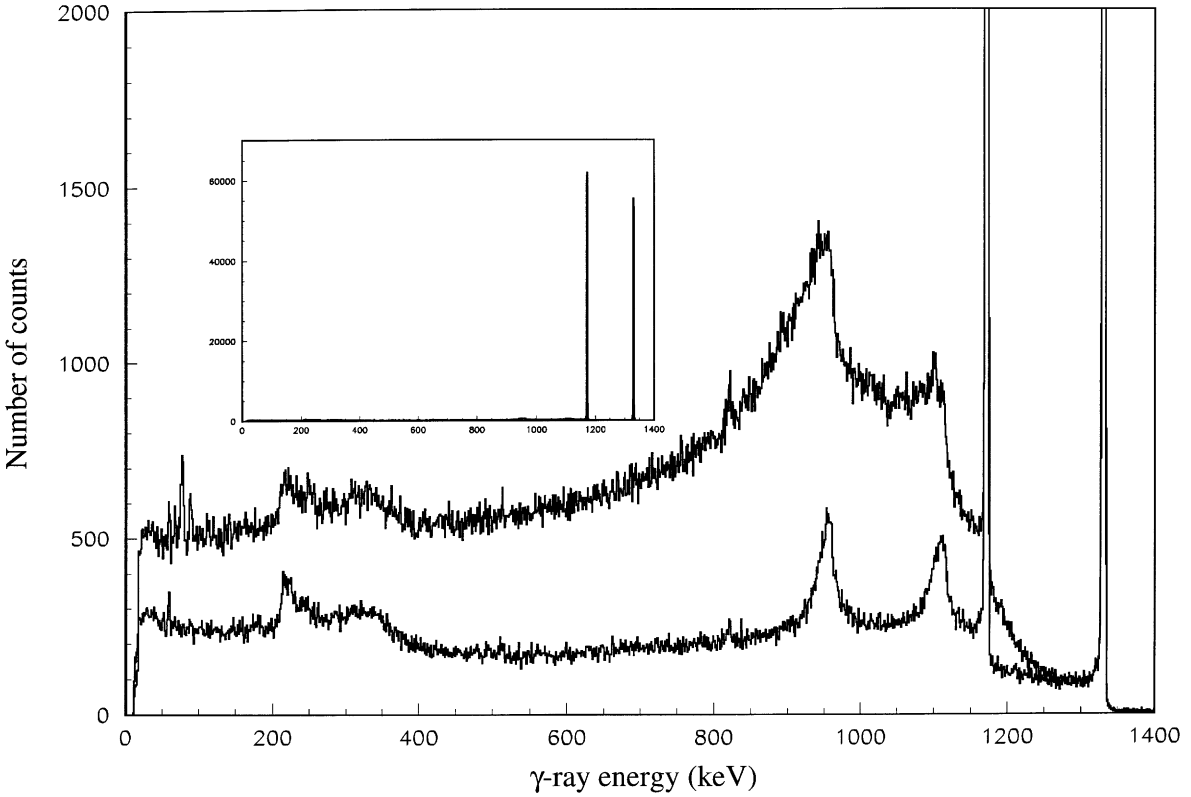

Fig. 6. Comparison between the unsuppressed spectrum obtained with a Clover detector and the suppressed spectrum measured with a Clover detector vetoed by its BGO suppression shield. The *y*-axis has been expanded to better appreciate the background reduction. The ^{60}Co source was placed at a distance to the front face of the Ge of 23 cm as in EUROGAM II. An indication of the quality of the suppressed spectrum is given in the insert which shows the photopeak versus background heights.

EUROGAM II. The parameters studied are the add-back factor, the Doppler broadening correction and the sensitivity of the Clover detector to the linear polarisation of γ transitions. These measurements have been performed at the Vivitron tandem accelerator of IReS, Strasbourg, using data collected in two different reactions.

One of the reactions was ^{125}Te(^{34}S,5n)^{154}Er at a bombarding energy of 176 MeV. The target was a stack of two foils of thickness 300 and 400 μg/cm^2, respectively, each evaporated on a gold backing (of thickness ~ 40 μg/cm^2) and covered on the other side by a thin gold film (of thickness ~ 40 μg/cm^2) to prevent Te evaporation. The residues formed in the reaction recoiled in vacuum with 2.2% of the velocity of light. Multiple coincidences with folds ≥ 3 were collected in a half day run.

The second reaction used was ^{124}Sn(^{30}Si, 5n)^{149}Gd at a beam energy of 160 MeV. In this case a stack of two thin self supporting Sn foils of thickness 430 and 500 μg/cm^2 respectively was used as target. The data were collected in a 10 day run.

5.2. Add-back factor

Gamma-rays from a ^{152}Eu source at the target position were recorded prior to the in-beam experiments. The mean add-back factor F value measured at 1408 keV is 1.52(2) in agreement with the previous measurements (see Section 4.2). This result confirms that the add-back factor is not affected by

the solid angle reduction due to the presence of heavy-metal collimators.

In the source run, the counting rate in each Clover crystal was very low ($\sim$ 100 counts/s). During the ^{34}S beam test, the evaporation residues were populated at high spins leading to high γ-multiplicity events. In this case, the mean counting rate in each Clover element was of about 6000 counts/s and the multiple hit for gammas and neutrons probability was estimated to about 10%. Fig. 7 presents the source (full circles) and in-beam (open circles) add-back factor values measured versus γ-ray energy. The two sets of data exhibit the same behavior as expected.

5.3. Doppler broadening correction

The correction procedure described in Section 3.3 has been tested with the ^{124}Sn(^{30}Si,5n)^{149}Gd reaction at low (371.4 keV) and high (1060.7 keV) γ-ray energies. The former transition belongs to the normal deformed (ND) level scheme [33] and the latter to the ^{149}Gd yrast superdeformed (SD) band [34].

The background spectra and the spectra for the two transitions of interest were generated with the condition that they were in coincidence with, respectively, one or two transitions in the SD band. The recoil velocity associated to each γ-ray was deduced from the difference of their Doppler shifts in the two extreme rings of 5 tapered Ge detectors (22.4° and 157.6°). We found $\beta F_1(\tau) = 1.86(2)\%$ for 371.4 keV and $\beta F_2(\tau) = 2.00(2)\%$ for 1060.7 keV. Two sets of Doppler shift corrected spectra were produced for the ND and SD structures using the appropriate recoil velocities given above. In each case two Doppler shift correction methods were applied, the traditional one which uses a unique correction angle, the Clover angle, and the new one described in Section 3.3 which used three correction angles.

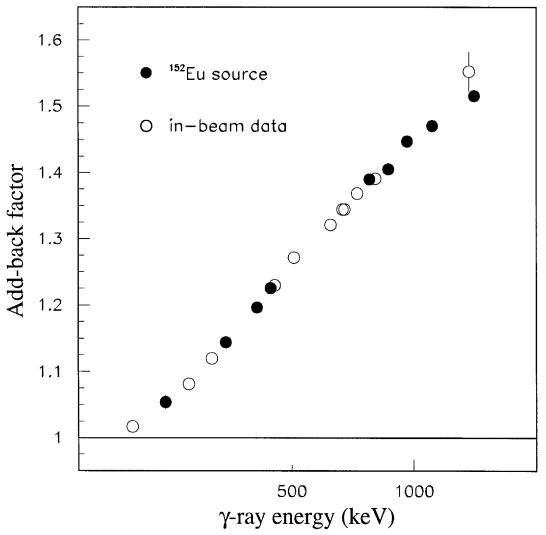

Fig. 7. Source (full circles) and in-beam (open circles) add-back factor values versus γ-ray energy measured in EUROGAM II. The error bars are generally smaller than the symbol size.

Fig. 8 shows the Doppler shift of the 1060.7 keV ^{149}Gd SD transition. The spectra a and c were measured with the upstream (a) and downstream (c) halfs of the Clover detectors. Spectrum (b) is the add-back spectrum corresponding to the coincidences between the two halfs. These three spectra were Doppler shift corrected by using the Clover angle. The peak centroids differ by $\sim$ 1.6 keV between spectra a and b and b and c. The sum spectra corresponding to the addition of the a,b and c contributions are obtained by applying a Doppler shift correction procedure using the Clover angle (Fig. 8(d), one angle correction) or the three angles of the a–c components (Fig. 8(e)). The FWHM of the sum peak in the one angle correction method is much wider than the one obtained with the three angles correction procedure. It is mainly governed by the different Doppler shifts of the three contributions a–c. The three angles correction method produces a spectrum that looks similar to that of a single Clover half.

Table 4 displays the FWHM and FWTM measured in the two sets of spectra for the 371.4 and 1060.7 keV transitions. A good agreement between the measured values and the predictions of the simulation calculations is found.

The FWHM values of the 1060.7 keV transition (see Fig. 8 and Table 4) show clearly the effect of the larger opening angle accessible to the coincidence events. Energy resolutions of about 3.8 and 4.5 keV are measured, respectively, in each half of the Clover detector and for coincidence events between the two halfs. The increase of only 0.7 keV between

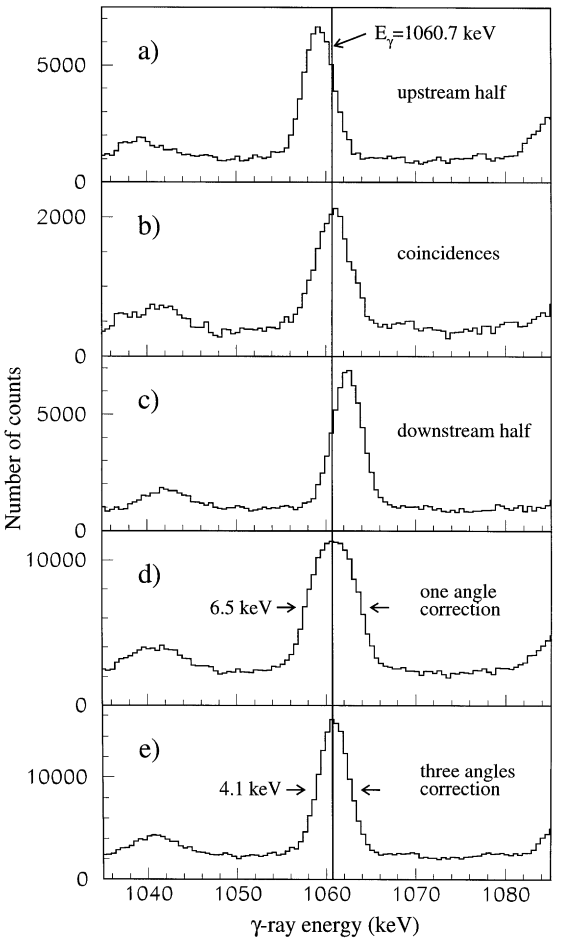

Fig. 8. Doppler shifts, Doppler broadening and line shape of the 1060.7 keV transition detected in the Clover detectors of EUROGAM II in the ^{124}Sn(^{30}Si,5n)^{149}Gd reaction. The spectra a and c were measured with the upstream (a) and downstream (c) Clover detector halfs. Spectrum (b) is the add-back spectrum for the coincidences between the two halfs. The sum spectra corresponding to the addition of the a, b and c contributions were obtained by applying a Doppler shift correction procedure using the Clover angle (d) or the three angles of the a to c components (e) (see Section 3.3). The FWHM values obtained in the total detection mode using the one angle (d) and the three angles (e) corrections are also reported.

these two values confirms however the predictions of the simulation calculations which show that the Compton scatterings are concentrated around the separation surface of the two Clover halfs (see Fig. 2). As a consequence, the FWHM of the coincidences (4.5 keV) is much smaller than the one corresponding to the full Clover opening angle (6.5 keV). The consecutive gain in peak height leads to larger signal-to-noise ratio and multidetector resolving power. Finally, the three angles correction procedure is also efficient on the FWTMs. The FWHM improvement observed between the two Doppler shift correction procedures would be much larger for higher transition energies and recoil velocities.

5.4. Polarisation measurements

In heavy-ion reactions, some of the magnetic substates of the nuclear excited levels are preferentially populated which leads to a nuclear alignment. This effect induces the anisotropy of the angular distribution and the linear polarisation of the γ-ray transitions deexciting the aligned nuclear states [26,35]. The values of the angular distribution parameters a_2 and a_4 and of the polarisation P are related to the nuclear alignment and to the deexcitation γ cascade (spins and parities of the levels involved, transition multipolarity, mixing ratios, …). The polarisation P can be measured by use of a special detector, the Compton polarimeter [36–40].

Since 1973, the linear Compton polarimeters use basically three Ge crystals, one scatterer and two absorbers [38]. The scatterer and one absorber crystals define the reaction plan which is parallel to the beam axis and the other absorber diode defines with the scatterer the vertical plan. Such a detector can be used to determine the electric or magnetic character of a γ-ray as electric (magnetic) transitions favour perpendicular (parallel) Compton scatterings [41].

In a Clover detector, each of the individual crystals can be considered as a scatterer and the two adjacent detectors as the absorbers. Thus a Clover detector corresponds to four conventional polarimeters in one cryostat. Of course, its sensitivity to the polarisation of the γ transitions will be reduced due to the close packing of the crystals. Our goal here was to prove the feasibility of such measurements with Clover detectors.

The polarisation sensitivity Q of a polarimeter is defined [26] as

$$Q = \frac{1}{P}\frac{N_\perp - N_\parallel}{N_\perp + N_\parallel} = \frac{A}{P} \tag{10}$$

Table 4
Doppler broadening correction. FWHM and FWTM in keV measured with EUROGAM II for two γ-ray energies. The data from the third to the sixth columns were obtained using a Doppler shift correction based on the traditional method which uses a unique correction angle, the Clover angle. In the last column, the angles of each components (downstream, upstream and coincidences) are taken into account. The experimental recoil velocity β corresponding to each transition is given in column two. Calculated FWHM values are also presented. The relative FWHM and FWTM accuracies are respectively $\sim 3\%$ and $\sim 5\%$

E_γ (keV)	β (%)		Downstream half	Upstream half	Halfs coinc.	One angle correction	Three angles correction
371.4	1.86 (2)	FWHM	2.6 (1)	2.6 (1)	3.0 (1)	3.0 (1)	2.6 (1)
		$FWHM_{calc}$	2.4	2.4	3.0	2.9	2.5
		FWTM	5.1 (3)	5.1 (3)	6.2 (3)	5.6 (3)	5.1 (3)
1060.7	2.00 (2)	FWHM	3.8 (1)	3.9 (1)	4.5 (2)	6.5 (2)	4.1 (2)
		$FWHM_{calc}$	4.2	4.2	4.6	6.4	4.4
		FWTM	7.4 (4)	7.4 (4)	8.7 (5)	10.2 (5)	7.6 (4)

P is the linear polarisation of the γ-ray detected, A the scattering assymetry, $N_\parallel$ and $N_\perp$ being the normalized counting rates observed respectively for the coincidences between the scatterer and the horizontal absorber and between the scatterer and the vertical absorber. The counting rates are normalised by a geometrical factor $a(E_\gamma)$ [38] to correct for the geometrical asymmetries of the polarimeter crystals. The normalisation factor is measured versus γ-ray energy in absence of polarisation. This can be performed with radioactive sources or in in-beam experiments measuring $N_\parallel$ and $N_\perp$ with the polarimeter placed at 0° to the beam axis.

The polarisation P depends on the multipolarity of the detected γ-ray, on the alignment of the emitting nuclear state and varies with $\sin^2\theta$ where θ is the detection angle to the beam axis. Its value is therefore maximum at 90° . When the radiation is a pure transition like an E2, the value of the polarisation can be deduced from the angular distribution coefficients. This fact is used to calibrate polarimeters, i.e. to determine their polarisation sensitivity Q. For that purpose angular distribution and linear polarisation of pure E2 transitions have to be measured over a wide range of γ energies.

The polarisation sensitivity of a polarimeter depends on its geometry. It can be calculated by use of the Klein–Nishina formula [41] which is integrated over all possible scattering angles. The closer the absorbers and scatterer crystals, the larger the scattering angle range and the smaller the polarisation sensitivity.

The ideal polarimeter would be a pointlike (pt) polarimeter which polarisation sensitivity Q_{pt} is calculated with the formula

$$Q_{pt}(\alpha) = \frac{1+\alpha}{1+\alpha+\alpha^2} \quad \text{with } \alpha = \frac{E_\gamma}{m_o c^2} \tag{11}$$

m_o is the electron mass.

The experimental polarisation sensitivity values Q_{exp} of a finite crystal size detector is generally fitted by the expression for a pointlike polarimeter reduced by a scaling factor

$$Q_{exp}(E_\gamma) = Q_{pt}(E_\gamma)(b_1 E_\gamma + b_0). \tag{12}$$

The quality of a polarimeter depends not only on its sensitivity to the polarisation but also on its detection efficiency [26,42]:

$$\varepsilon_c(E_\gamma) = \frac{(N_\parallel + N_\perp)/2}{N_{tot}} . \varepsilon_p \omega(E_\gamma) \tag{13}$$

where N_{tot} is the total number of γ-rays with the energy E_γ detected during the measurement and $\varepsilon_p\omega$ is the absolute photopeak efficiency of the polarimeter at the γ-ray energy E_γ. The polarisation sensitivity Q is improved to the detriment of the coincidence efficiency ε_c by increasing the distance between the scatterer and the absorber crystals. As a consequence, a compromise between polarisation

sensitivity and coincidence efficiency has to be found to allow the polarisation measurements of low intensity transitions. The figure of merit FM of a Compton polarimeter takes this double dependence into account. It can be written as [26,43]:

$$\mathrm{FM} = Q^2.\varepsilon_c \tag{14}$$

and is commonly used to compare the performance of various polarimeters.

5.4.1. Polarisation sensitivity Q. Calibration of the Clover detector

The Clover detector has been calibrated as a Compton polarimeter. We used (p,p'γ) reactions on ^{19}F, ^{nat}Ag, ^{56}Fe and ^{24}Mg with incident proton energies in the range 2.4–3.0 MeV to provide five polarised pure stretched E2 transitions of energy 197, 418 and 423, 845 and 1368 keV, respectively [26,37,38,42]. The Clover detector was placed at 90° relative to the beam axis for the polarisation measurements and at 0° to determine the geometrical factor $a(E_\gamma)$. The γ-ray polarisation P was deduced from the angular distribution data [26,35].

The experimental polarisation sensitivity values Q_{exp} for the Clover detector are shown in Fig. 9 along with the values measured using two other Compton polarimeters, a three Ge(Li) detector made of three separate crystals [38] and the segmented polarimeter, a single 20% relative efficiency crystal whose external contact is electrically segmented in height regions parallel to the crystal axis [42]. The "*c* configuration" of the latter polarimeter is similar to the Clover detector geometry. The curves were fitted using Eq. (12). For the Clover detector we found $b_0 = 0.29 \pm 0.03$ and $b_1 = 0.0 \pm 0.003$. The calibration procedure is detailed in Refs. [23,44]. Despite its very compact geometry, the Clover detector is still sensitive to the linear polarisation.

In Table 5 are reported the polarisation sensitivity, the coincidence efficiency ε_c and the figure of merit FM measured at 1368 keV with the three polarimeters mentioned above. Due to its very large coincidence efficiency, the Clover detector is by far the best polarimeter for γ-rays of weak intensities. This effect is confirmed by simulation calculations performed by Garcia-Raffi et al. using the code GEANT 3 [45].

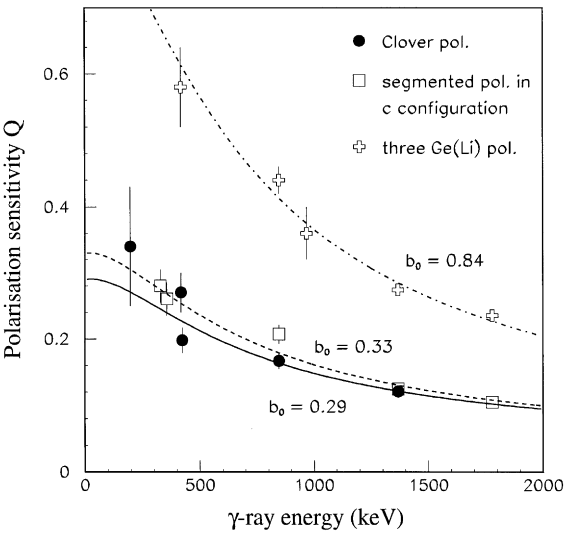

Fig. 9. Polarisation sensitivity Q versus γ-ray energy of three different polarimeters: the Clover detector (present work, full circles), the segmented polarimeter in the "c configuration" ([42], open squares) and the three Ge(Li) polarimeter ([38], crosses). The experimental data are shown along with the sensitivity of a pointlike polarimeter scaled by a coefficient b_0 (curves).

Table 5
Values of polarisation sensitivity Q, coincidence efficiency ε_c and figure of merit FM measured at 1368 keV with three different polarimeters

	Q	ε_c ($\times 10^4$)	FM ($\times 10^8$)
Three Ge(Li)	0.274 (7)[a]	0.037 (2)	28 (2)
Segmented detector[b]	0.14 (1)	0.24 (1)	47 (5)
Clover detector	0.121 (5)	2.33 (7)	341 (23)

[a] Ref. [38].
[b] c configuration in Ref. [42].

5.4.2. Polarisation measurement with EUROGAM II

We have used the Clover detectors in EUROGAM II to measure the linear polarisation of γ-rays emitted in the ^{125}Te(^{34}S,5n)^{154}Er heavy-ion reaction. In the EUROGAM the Clover detectors are positioned in the angular range where the polarisation P is maximum.

The geometrical factor a (E_γ) has been measured for the 24 Clover detectors using a ^{152}Eu source. As

expected, this quantity is found to be photon energy independent and close to 1 ($a = 1.03(2)$).

Fig. 10 shows γ-ray radiations of energy 668.8 and 675.5 keV measured with the EUROGAM Clover detectors. The former is a pure stretched E2 transition while the latter is a mixed $\Delta I = 1$, M1 + E2 transition. In order to improve the statistics, the contribution of the 24 Clover detectors where summed after applying the three angles Doppler shift correction procedure. Spectra a and b correspond to the perpendicular and the parallel coincidences, respectively. The sensitivity of the Clover detector to the linear polarisation of γ-rays is directly visible in the coincidence spectra by comparing the relative peak heights of the two transitions. The difference between perpendicular and parallel coincidences shows directly the electric or magnetic nature of the transitions by, respectively, clear positive or negative peaks. Mixed transitions are less marked. Spectrum c is the difference of the coincidence spectra a and b. It confirms that the 668.8 keV γ-ray is an electric transition (positive) whereas the mixed 675.5 keV γ-ray appears slightly negative.

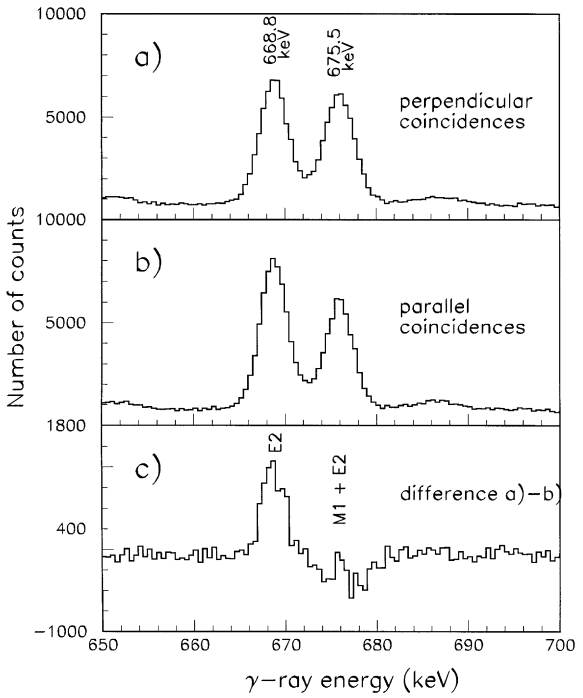

Fig. 10. Sum spectra of perpendicular (a) and parallel (b) coincidences. The 668.8 V and 675.5 keV γ rays correspond to a pure E2 transition and a mixed $\Delta I = 1$ M1 + E2 transition, respectively. The polarisation sensitivity of the Clover detector can directly be observed on spectrum c which is the difference of spectra a and b.

Several quantitative measurements have also been performed to calculate the polarisation P of various γ transitions in ^{154}Er nucleus by using the polarisation sensitivity curve of Fig. 9 with $b_0 = 0.29$. Some of these P values are given in Table 6. The relative γ intensities are taken from Ref. [46]. Most of the polarisation values from this work agree within the error bars with the data measured previously by Beck et al. [47] using a classical Compton polarimeter. The polarisation accuracy of the data obtained with EUROGAM is by a factor two smaller than the one of Ref. [47] (see Table 6) although the experiment lasted only 12 h. This demonstrates the high figure of merit and hence the power of the Clover detector as a Compton polarimeter. The large photopeak detection efficiency of EUROGAM allowed us to perform the analysis in triple coincidences. We required that at least two γ-ray energies in ^{154}Er were detected in any detector of the array when a two fold event in a Clover detector is detected. These gating conditions led to clean Clover coincidence spectra with large statistics, which, in spite of the modest polarisation sensitivity of the composite detector, allowed polarisation measurements for γ-rays of quite low relative intensity ($I_\gamma \sim 10\%$).

Polarisation measurements are essentially used to determine the parity of the state from which or to which the transition studied deexcites. For example in ^{154}Er, the dipolar transition 924.5 keV [46] deexcites a 34 $\hbar$ state with unknown parity lying at an excitation energy $E^\star = 11353.9$ keV towards a 33^- state with $E^\star = 10429.4$ keV ([46], Fig. 5). The measured polarisation value – 0.31(8) indicates that this transition is magnetic with a P value compatible with the theoretical one calculated for a pure M1 transition emitted by a state fully aligned (-0.35). Thus a negative parity is assigned to this 34 $\hbar$ state.

5.5. Neutron damage sensitivity

The sensitivity of Ge detectors to neutron damage is an important parameter for their use in large

Table 6
Relative γ intensity I_γ of ^{154}Er transitions [46], multipolarity nature of the transitions [47], measured scattering asymmetry A and polarisation sensitivity Q of the Clover detector deduced from Eqs. (11) and (12) with $b_0 = 0.29$. Are also given the state polarisation P deduced from the EUROGAM Clover data and the polarisation data $P_{[47]}$ published in Ref. [47]. These data were obtained from a short half day run

γ-ray energy (keV)	I_γ (%)	Nature	A	Q	P	$P_{[47]}$
279.2	41	E_1	0.084 (6)	0.24 (3)	0.35 (4)	0.35 (9)
318.3	88	E_2	0.095 (5)	0.23 (2)	0.41 (5)	0.36 (7)
321.3	10	E_2	0.15 (6)	0.23 (2)	0.6 (2)	–
455.6	94	E_2	0.072 (4)	0.20 (2)	0.36 (4)	0.13 (6)
506.9	97	E_2	0.061 (4)	0.19 (2)	0.32 (4)	0.28 (8)
668.8	98	E_2	0.057 (6)	0.17 (2)	0.34 (5)	0.35 (7)
726.7	85	E_2	0.072 (4)	0.16 (2)	0.45 (5)	0.25 (10)
805.0	100	E_2	0.048 (3)	0.15 (2)	0.32 (3)	0.30 (10)
827.5	49	E_2	0.06 (1)	0.15 (2)	0.40 (7)	0.48 (20)
919.7	19	E_2	0.086 (8)	0.13 (1)	0.66 (9)	–
924.5	25	M_1[a]	− 0.04 (1)	0.13 (1)	− 0.31 (8)	–
1368.8	12	E_2	0.06 (2)	0.10 (1)	0.6 (2)	–

[a]This work.

multidetector arrays. The increase of the Ge crystal diameter is associated to an increase of the sensitivity to neutron damage. The Clover detector which is composed of four modest diameter crystals (50 mm), should have an improved resistance to radiation damage as compared with tapered detectors (∼ 70 mm in diameter).

After two years experiments with EUROGAM II conclusions can be drawn concerning the relative sensitivity to neutron damage of the Clover detectors and the tapered counters. Absolute values are not available since no measurement of absolute neutron flux has been performed during the EUROGAM II experiments.

During the 210 beam days in EUROGAM II, 92 detectors have been annealed at IReS, Strasbourg, 63 tapered and 29 Clover detectors. The criterion to dismount a tapered counter from the array was a FWHM of the 1332 keV γ line larger than 3 keV and a FWTM/FWHM ratio larger than 2.1. For 50 mm diameter crystals, a low-energy tail appears on the low energy side of the photopeaks whereas their FWHM are only weakly affected by neutron damage. Thus we required for Clover detectors a FWHM between 2.5 and 2.8 keV and a FWTM/FWHM ratio of 2.0 to remove the counter from the array.

Let us define the neutron sensitivity ratio (NSR) as the tapered versus Clover detector neutron sensitivity:

$$\mathrm{NSR} = \left(\frac{\mathrm{N\ Tap\ A}}{\mathrm{N\ Tap\ M}}\right) \times \left(\frac{\mathrm{N\ Clo\ A}}{\mathrm{N\ Clo\ M}}\right)^{-1} \times \left(\frac{\mathrm{dTap}}{\mathrm{dClo}}\right)^{2} \times \mathrm{RF} \qquad (15)$$

where NTapA (NTapM) are the number of tapered detectors annealed (mounted on the array), NCloA (NCloM) are the number of Clover detectors annealed (mounted on the array), dTap (dClo) are the target-to-crystal distance on EUROGAM II for the tapered (Clover) detectors [9,12] and RF is a "recoil factor" which takes into account the focalisation of neutrons towards forward angles due to the kinematic of the reaction. The latter factor has been calculated using a recoil velocity averaged over all EUROGAM II experiments ($\beta \sim 2\%$) and an average neutron kinematic energy of 2 MeV. Knowing the detector distribution in the multidetector array (see Section 5.1) we obtain RF = 0.9. Although the Clover detector is handicapped by the neutron sensitivity dispersion of its four Ge crystals, the deduced NSR value (∼ 1.3) shows that the composite detector is markedly less sensitive than a tapered large volume detector.

6. Conclusion

In 1990, the scientific community was very sceptical of the novel idea to employ a composite Ge detector in a γ-ray multidetector array. However, based on GEANT 3 simulation calculations and several technical developments made by the Company Eurisys Mesures and us, the Clover detector was produced. This paper reports the performance measured with these new detectors in EUROGAM II.

The Clover detector is a composite detector consisting of four $\sim 21\%$ efficiency crystals mounted in a compact geometry. Working in the total detection mode, the photopeak detection efficiency of the Clover detector at 1332 keV is increased by a factor 1.52 (add-back factor) relative to the direct mode. The in-beam FWHM of γ lines can be improved significantly with Clover detectors by using their mechanical subdivision and an appropriate Doppler broadening correction method. The Clover detector can be used as a Compton polarimeter to measure the linear polarisation of γ-rays. Although its sensitivity to the linear polarisation is quite modest due to the compact crystal geometry, the large detection efficiency of the Clover detector leads to a figure of merit by a factor ~ 7 larger than previous germanium polarimeters. Finally, this composite detector is less sensitive to neutron damage by a factor ~ 1.3 than large volume detectors like the EUROGAM I tapered detectors. This is related to the use of moderate size crystals for the Clover detector.

The Clover detector completely fulfilled the simulated and expected characteristics and properties which led the France-UK collaboration to equip EUROGAM II with 24 such Compton suppressed counters.

7. For Further Reading:

The following reference is also of interest to the reader: [39].

Acknowledgements

The authors acknowledge the Company Eurisys Mesures for its efficient collaboration in the development, the improvement and the serial production of the Clover detectors. This work was supported by the EPSRC (U.K.) and the IN2P3 (France).

References

[1] H. Morinaga, P.C. Gugelot, Nucl. Phys. 46 (1963) 210.
[2] A. Johnson, H. Ryde, J. Sztarkier, Phys. Lett. B 34 (1971) 605.
[3] F.A. Beck, in: D. Shapira (Ed.), Proc. Conf. on Instrumentation for Heavy Ion Nuclear Research, ed. Nucl. Sci. Research Conf. Series, Vol. 7, Harwood, New York, 1984, p. 129.
[4] P.J. Nolan, D.W. Gifford, P.J. Twin, Nucl. Instr. and Meth. A 236 (1985) 95.
[5] P.J. Twin et al., Nucl. Phys. A 409 (1983) 343c.
[6] P.J. Twin et al., Phys. Rev. Lett. 57 (1986) 811.
[7] Th. Byrski et al., Phys. Rev. Lett. 64 (1990) 1650.
[8] C.W. Beausang, J. Simpson, J. Phys. G 22 (1996) 527.
[9] P.J. Nolan, F.A. Beck, D.B. Fossan, Annu. Rev. Nucl. Part. Sci. 45 (1994) 561.
[10] C. Rossi-Alvarez, Nucl. Phys. News Europe 3 (3) (1993) 10.
[11] D. Bazzacco, Workshop on Large Gamma-Ray Detector Arrays, Chalk River, Canada, AECL 10613, 1992, p. 376.
[12] F.A. Beck, Prog. Part. Nucl. Phys. 28 (1992) 443.
[13] C.W. Beausang et al., Nucl. Instr. and Meth. A 313 (1992) 37.
[14] J. Gerl, R.M. Lieder (Eds.), EUROBALL III, European γ-ray facility, GSI Darmstadt, 1992.
[15] F.A. Beck et al., Nucl. Phys. A 557 (1993) 67c.
[16] G. de France et al., Phys. Rev. C 53 (1996) R1070.
[17] D.S. Haslip et al., Phys. Rev. Lett. 78 (1997) 3447.
[18] T.L. Khoo et al., Phys. Rev. Lett. 76 (1996) 1583.
[19] A. Lopez-Martens et al., Phys. Lett. B 380 (1996) 18.
[20] Ch. Finck et al., Phys. Lett. B, submitted for publication.
[21] G. Duchêne et al., Workshop on Large Gamma-ray Detector Arrays, Chalk River, Canada, AECL 10613, 1992, p. 359 and p. 364.
[22] F.A. Beck, Conf. on Phys. from Large γ-Ray Detector Arrays, Berkeley, USA, LBL 35687, vol. 2, 1994, p. 154.
[23] L. Han, Ph.D. Thesis, ULP Strasbourg, CRN 95-24, 1995.
[24] J. Eberth, H.G. Thomas, P.v. Brentano, R.M. Lieder, H.M. Jäger, H. Kämmerling, M. Berst, D. Gutknecht, R. Henck, Nucl. Instr. and Meth. A 369 (1996) 135.
[25] GEANT, version 3.159; R. Brun, F. Bruyant, M. Maire, A.C. McPherson, P. Zanarini, GEANT3 User's Guide, DD/EE/84-1, CERN, 1987.
[26] F.A. Beck, Ann. Phys. (Paris) 1 (1966) 503.
[27] G. de France, Ph.D. Thesis, ULP Strasbourg, CRN 91-21, 1991.
[28] R. Wyss, Nucl. Instr. and Meth. A 256 (1987) 499.

[29] K. Spohr et al., Acta Phys. Polonica B 26 (2-3) (1995) 297.
[30] S. Lenzi et al., Phys. Rev. C 56 (1997) 1313.
[31] M. Moszynski, G. Duchêne, Nucl. Instr. and Meth. A 308 (1991) 557.
[32] C. Michel, H. Emling, E. Grosse, F. Azgui, H. Grein, H.J. Wollersheim, J.J. Gaardhøje, B. Herskind, Nucl. Instr. and Meth. A 251 (1986) 119.
[33] S. Flibotte, B. Haas, F. Banville, J. Gascon, P. Taras, H.R. Andrews, D.C. Radford, D. Ward, J.C. Waddington, Nucl. Phys. A 530 (1991) 187.
[34] S. Flibotte et al., Nucl. Phys. A 584 (1995) 373.
[35] P.J. Twin, in: W.D. Hamilton, The Electromagnetic Interaction in Nuclear Spectroscopy, North-Holland Pub. Co-Amsterdam, 1975, p. 701.
[36] C. Broude, O. Husser, H. Malm, J.F. Sharpey-Schafer, T.K. Alexander, Nucl. Instr. and Meth. 69 (1969) 29.
[37] R. Bass, S. Brinkmann, C. von Charzewski, H. Hanle, Nucl. Instr. and Meth. 104 (1972) 33.
[38] P.A. Butler, P.E. Carr, L.L. Gadeken, A.N. James, P.J. Nolan, J.F. Sharpey-Schafer, P.J. Twin, D.A. Viggars, Nucl. Instr. and Meth. 108 (1973) 497.
[39] K. Ashibe, M. Adachi, H. Taketani, Nucl. Instr. and Meth. 130 (1975) 221.
[40] S. Ohya, H. Miura, K. Nishimura, N. Mutsuro, Nucl. Instr. and Meth. A 276 (1989) 223.
[41] O. Klein, Y. Nishina, Z. Phys. 52 (1929) 853.
[42] J. Simpson, P.A. Butler, L.P. Ekström, Nucl. Instr. and Meth. 204 (1983) 463.
[43] B.A. Logan, R.T. Jones, A. Ljubicic, Nucl. Instr. and Meth. 108 (1973) 603.
[44] P. Jones et al., Nucl. Instr. and Meth. A 362 (1995) 556.
[45] L.M. Garcia-Raffi, J.L. Tain, J. Bea, A. Gadea, J. Rico, B. Rubio, Nucl. Instr. and Meth. A 391 (1997) 461.
[46] C. Schück, M.A. Deleplanque, R.M. Diamond, F.S. Stephens, J. Dudek, Nucl. Phys. A 496 (1989) 385.
[47] F.A. Beck et al., Z. Phys. A 319 (1984) 119.